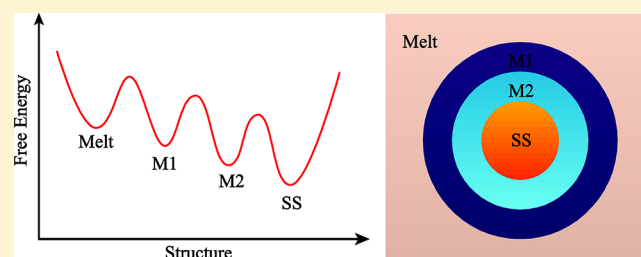


Nucleation of a Stable Solid from Melt in the Presence of Multiple Metastable Intermediate Phases: Wetting, Ostwald's Step Rule, and Vanishing Polymorphs

Mantu Santra, Rakesh S. Singh, and Biman Bagchi*

Solid State and Structural Chemistry Unit, Indian Institute of Science, Bangalore 560012, India

ABSTRACT: In many systems, nucleation of a stable solid may occur in the presence of other (often more than one) metastable phases. These may be polymorphic solids or even liquid phases. Sometimes, the metastable phase might have a lower free energy minimum than the liquid but higher than the stable-solid-phase minimum and have characteristics in between the parent liquid and the globally stable solid phase. In such cases, nucleation of the solid phase from the melt may be facilitated by the metastable phase because the latter can “wet” the interface between the parent and the daughter phases, even though there may be no signature of the existence of metastable phase in the thermodynamic properties of the parent liquid and the stable solid phase. Straightforward application of classical nucleation theory (CNT) is flawed here as it overestimates the nucleation barrier because surface tension is overestimated (by neglecting the metastable phases of intermediate order) while the thermodynamic free energy gap between daughter and parent phases remains unchanged. In this work, we discuss a density functional theory (DFT)-based statistical mechanical approach to explore and quantify such facilitation. We construct a simple order-parameter-dependent free energy surface that we then use in DFT to calculate (i) the order parameter profile, (ii) the overall nucleation free energy barrier, and (iii) the surface tension between the parent liquid and the metastable solid and also parent liquid and stable solid phases. The theory indeed finds that the nucleation free energy barrier can decrease significantly in the presence of wetting. This approach can provide a microscopic explanation of the Ostwald step rule and the well-known phenomenon of “disappearing polymorphs” that depends on temperature and other thermodynamic conditions. Theory reveals a diverse scenario for phase transformation kinetics, some of which may be explored via modern nanoscopic synthetic methods.



1. INTRODUCTION

In the random first-order transition (RFOT) theory of glass transition developed by Kirkpatrick, Thirumalai and Wolynes (KTW) and Xia and Wolynes (XW),¹ nucleation of a liquid droplet within a glass/amorphous phase was proposed as the basic relaxation mechanism. The authors employed an unusual size dependence of the surface tension in the form of $\gamma(R) = \gamma_0/R^{1/2}$, where $\gamma(R)$ is the size (R) dependent surface tension of the droplet–glass interface. While curvature dependence of surface tension is often derived in terms of Tolman's length, this dependence has a completely different origin. This square root dependence comes from the idea of a random Ising model where the nucleus of a new phase can be wetted by many phases of intermediate (between daughter and parent phases) order.

When this unusual square root dependence of the surface tension is substituted back into classical nucleation theory (CNT), it gives rise to the well-known Adam–Gibbs (AG)² relation between the relaxation time and configurational entropy (s_c), thus providing a simple and elegant derivation of this famous relationship. The original derivations of AG and many subsequent studies have focused on the cooperatively rearranging regions (CRRs) that form the basis of the AG

relation. These CRRs are often identified with a correlation length in a deeply supercooled liquid. In the AG picture, the size of the CRR increases rapidly as the liquid approaches the glass transition and the configurational entropy approaches zero. In the KTW and XW treatment,¹ the size of the critical nucleus grows as $s_c^{-2/3}$ as the configurational entropy (s_c) decreases. However, the derivation of Xia and Wolynes^{1b} apparently does not require such a growing correlation length; this picture is quite different and based on the ideas of nucleation and first-order phase transitions.

However, the peculiar size dependence of the surface tension has not been investigated in detail. As mentioned in one of the preceding paragraphs, the peculiar size dependence arises by invoking the concept of “wetting” of the interface between the growing liquid and the parent glass. The concept of wetting is a well-known phenomenon, and it plays a direct or indirect role in many theoretical studies and has been often observed

Special Issue: Peter G. Wolynes Festschrift

Received: March 29, 2013

Revised: May 16, 2013

experimentally and in computer simulation studies.^{3–8} For example, a face-centered cubic (fcc) solid phase may form where the body-centered cubic (bcc) solid remains a metastable solid (MS) phase.

In this paper, we shall take the cue from Xia and Wolynes^{1b} but employ density functional theory (DFT) to study the effect of an intermediate phase on the nucleation and growth scenario in complex systems. We demonstrate that wetting of the interface by phases of intermediate order can dramatically reduce the value of the surface tension, and under certain conditions, the surface tension decreases inversely with the number of phases.

In an elegant application of irreversible thermodynamics, van Santen⁹ showed that the formation of the stable phase is facilitated by the presence of intermediate phases. This is intimately connected with the Ostwald step rule (OSR).^{10,11} This quantifies the condition under which different phases will appear.

Ostwald argued that the formation of a phase is not determined by its absolute stability but by the closeness of the growing phase to the parent phase.¹⁰ Although Ostwald did not mention it explicitly, what he meant by “closeness” is that the surface tension determines the growth. A demonstration of this fact comes from critical phenomena where surface tension varies as $\gamma \approx (\Delta\rho)^4$.

Thus, we see that two very different problems in the area of scientific research (namely, the glass transition and the synthesis of solids) can be related very intimately. The formation of a new solid is often wetted by MSs to lower surface tension. The intermediate phase can be metastable with respect to either both solid phases or only the final solid (in the case of crystallization) and liquid (in the case of the glass transition). Additionally, the number of phases involved in wetting can have dramatic effects. In a highly interesting study, Granasy and Oxtoby¹² already observed this scenario in the presence of one metastable phase. Although they did not mention the OSR explicitly (surprising omission), their analysis essentially provides a beautiful elucidation of the condition underlying the validity of the OSR. However, Granasy and Oxtoby¹² considered one metastable intermediate phase that distinguishes their work from the work of Xia and Wolynes,^{1b} who had multiple phases wetting the interface.

Intervention by multiple intermediate phases lowers the surface tension; the unusual $1/\sqrt{R}$ is not clear yet. Such a relation can be rigorously valid only asymptotically and can require a very broad interface such that many intermediate phases can be accommodated. Granasy and Oxtoby¹² did observe the conditions where the interface becomes very broad, and it is also observed that the surface tension decreases with the width of the interface as $\gamma \approx 1/w^2$ (without wetting);¹³ one would naturally suspect that the Xia–Wolynes expression could be valid under certain conditions, which need to be explored in detail.

Furthermore, protein folding and crystallization from melt to solids with multiple polymorphs, the two phenomena of current interest in biology and materials science, share a common physical chemistry basis. Both have a similar rugged energy landscape arising from definite entropy–enthalpy relationships.^{14–16} The energy landscape paradigm of condensed matter science^{15,17,18} assumes the existence of multiple free energy minima in the configurational space, with the minima (in principle) being multiply connected. Transition between such minima is described in terms of free energy

barriers along a chosen path. We discuss here that the choice of the efficient path can be dictated by thermodynamic conditions. Therefore, thermodynamics (free energy minima) and kinetics (barriers) are intimately correlated in the energy landscape.

In the case of crystallization of a solid from a liquid or melt, we need order parameters that uniquely identify different structures. That is, ideally, each minimum should be characterized by a set of values of the order parameters and should correspond to a unique structure. In the Ramakrishnan–Yusouff DFT of freezing,¹⁹ the order parameters are the density components evaluated at the reciprocal lattice vectors of the solid, along with the fractional density change. It is relatively easy to make either an equilibrium or a dynamic calculation of freezing to different lattice types. That is, one can explain why argon freezes into a fcc lattice while liquid sodium freezes into a bcc solid. However, the situation is far more difficult in the case of complex solids like zeolites.²⁰ Here, we do not have the information about the liquid structure necessary for a microscopic theory.

An elegant illustrative example of the OSR was recently provided in the formation of the thermodynamically stable crystalline form of LiFePO_4 (olivine structure) via multiple metastable intermediate crystalline phases.¹⁶ In the energy landscape picture, the surface tension and difference between the minimum of the free energy corresponding to two structures play important roles in determining the nucleation barrier between two metastable phases or one metastable and one stable solid (SS) phase. However, it is very hard to obtain the surface tension between two MS phases.

In the energy landscape view, the polymorphs are the inherent structures of the sol phase and should be obtained when the vibrational degrees of freedom and the kinetic energy are removed from the molecules. Thus, the polymorphs form a rugged landscape with the most stable structure at the bottom of the energy ladder, just like the rugged folding funnel of a protein developed by Onuchic, Wolynes, and co-workers.¹⁵

When we consider the formation of the MS (which we assume to be the closest to the sol phase), then the free energy gap ΔG_V is lower than the most stable phase referred to as the SS. Thus, according to CNT,^{21–26} the only way that the phase MS can precipitate out at any temperature is to have such a lower surface tension that the nucleation barrier is the lowest for MS. Because of the lower solid–liquid surface tension leading to a lower nucleation barrier, MSs are kinetically favored. Thus, kinetics seems to play a very dominant role. We must note that even in simple systems, the validity of CNT (at least at high supersaturation) itself is questionable.^{27–32}

At high temperature, the following proposed scenario holds. Because the energy of the system is high, it can probe all of the minima of the system. Even if it gets trapped in a low-lying minimum, like in the M1 or M2 phase, it can escape from the minimum before the phase grows to macroscopic size. In other words, when the nucleus forms, it can melt within a time comparable to the relaxation time of the system. It of course gets trapped many times in the low-lying minima and gets out again and again. When it gets trapped in the deep minimum of the most stable phase, it can grow. However, when the temperature is low, it gets trapped in the closest minimum as envisaged by Ostwald.

In the next section, we construct a DFT that provides a quantitative explanation of the sequential formation of metastable states before transforming to the most stable phase.

2. ONE METASTABLE INTERMEDIATE PHASE: DFT OF THE SURFACE TENSION AND NUCLEATION BARRIER

The classical DFT was introduced by Lebowitz and Percus³³ and Stillinger and Buff³⁴ and has been advanced by many others in the last 5 decades.^{35–38} Oxtoby and co-workers extensively applied the DFT to study the nucleation processes in many simple and complex systems.^{36–38} In this work, first we shall discuss the one order parameter description to bring out the generality of the problem, and then, a two order parameter description is provided. In the next section, we shall describe the DFT of the surface tension and nucleation barrier in the presence of one metastable intermediate phase. This case has close resemblance to the study of Granasy and Oxtoby.¹² A schematic representation of the free energy surface is provided in Figure 1.

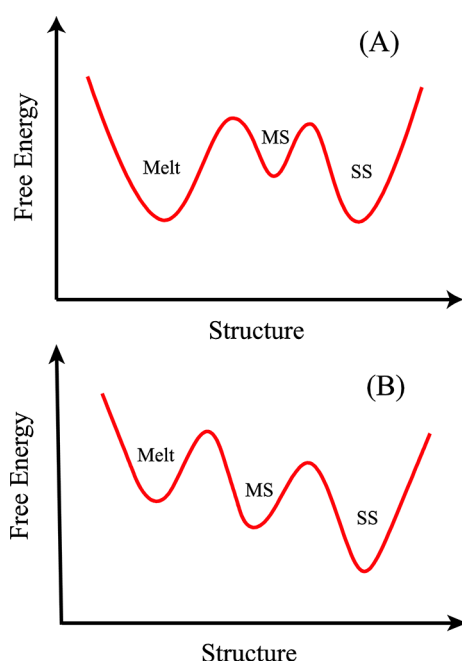


Figure 1. Schematic free energy landscape of crystallization of the SS from the melt in the presence of a MS phase. (A) The case when the melt and SS phases are at coexistence and the intermediate phase is metastable with respect to both (melt and SS). (B) The case when the intermediate phase is stable with respect to melt but metastable with respect to the global SS phase.

A. Numerical Implementation of the Effects of Wetting within a One Order Parameter Theory. The ideas articulated in the previous section can be nicely verified within a one order parameter theory, using DFT. The proposed free energy functional for three phases, the low-density melt, intermediate MS phase, and high-density SS phase are

$$\Omega_i[\rho(\mathbf{r})] = \int d\mathbf{r} [f_i(\rho(\mathbf{r})) - \mu\rho(\mathbf{r})] + \frac{1}{2} \int d\mathbf{r} [K_\rho(\nabla\rho(\mathbf{r}))^2] \quad (1)$$

where f_i is local Helmholtz free energy density function of the average number density $\rho(\mathbf{r})$ of the i th phase and μ is the chemical potential. Here, i indicates respective phases as $i = M$ stands for melt, $i = MS$ for intermediate solid, and $i = SS$ for stable solid phase. The last term (square gradient term)

accounts for the nonlocal effects in the system due to inhomogeneity in the density order parameter. K_ρ is related to the density correlation length. The Helmholtz free energy density for each phase is

$$f_i(\rho) = a_i(\rho - \rho_i)^2 + f_{i,0} \quad (2)$$

where $i = M$ for melt, MS for the metastable solid, and SS for the stable solid phase. The value of the parameters are $a_M = 1500$, $a_{MS} = 2000$, and $a_{SS} = 2500$, the equilibrium densities are $\rho_M = 0.88$, $\rho_{MS} = 0.97$, $\rho_{SS} = 1.05$, and $f_{M,0} = 0.0$, $f_{SS,0} = 0.80$, and $f_{MS,0}$ is varied from 0.6 to 20.0.

B. Surface Tension. In order to get the surface tension between coexisting phases, first we need to get the equilibrium densities of coexisting phases. This can be determined by equating the chemical potential and thermodynamic grand potential density (pressure) of two phases.

$$\mu_\alpha(\rho_\alpha) = \mu_\beta(\rho_\beta) \quad \text{and} \quad \omega_\alpha(\rho_\alpha) = \omega_\beta(\rho_\beta) \quad \text{where} \\ \mu_i = \left(\frac{\partial f_i(\rho)}{\partial \rho} \right)_T \quad \text{and} \quad \omega_i = f_i - \mu_i \rho_i \quad (3)$$

The above two conditions ensure that the system is in both thermodynamic and mechanical equilibrium.

We can evaluate the values of the surface tension between the coexisting phases for a planar interface along the z -axis by solving the Euler–Lagrange equations associated with following equilibrium conditions

$$\frac{\delta \Omega[\rho(z)]}{\delta \rho(z)} = 0 \quad (4)$$

where $\Omega[\rho(z)]$ is the grand canonical free energy functional corresponding to the inhomogeneous system with density profile $\rho(z)$

$$\Omega[\rho(z)] = \int dz [f(\rho(z)) - \mu\rho(z)] + \frac{1}{2} \int dz [K_\rho(\nabla\rho(z))^2] \quad (5)$$

where $f = \min\{f_i\}$.

The density profiles shown in Figure 2A are obtained by solving the corresponding Euler–Lagrange equation (eq 4) under appropriate boundary conditions. The surface tension is the extra energy cost for the formation of an interface and is defined as

$$\gamma_{M-SS} = \frac{(\Omega(\rho(z)) - \Omega_{M/SS})}{A} \quad (6)$$

where $\Omega_{M/SS}$ is the free energy of the coexisting melt and high-density SS phase and A is the area of the interface.

In order to study the effect of the intermediate phase on the density profile and surface tension, the melt and SS phases are kept at coexistence, and the stability of the intermediate phase ($\Delta\omega_{MS}$) is gradually varied. After inserting the equilibrium density profiles in eq 5, the calculated surface tensions (using eq 6) are shown in Figure 2B. We note the strong dependence of the surface tension on the extent of metastability of the intermediate phase. As the difference between the minimum of free energy basins between the melt and intermediate phase decreases, the effect of wetting becomes more pronounced. This is reflected in both the density profile as well as surface tension. We note the significant decrease in the interfacial

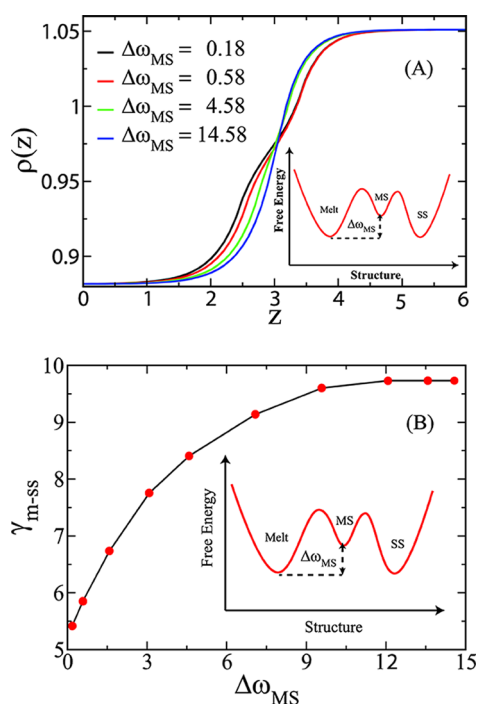


Figure 2. (A) The calculated density profiles between the coexisting low-density phase (melt) and the high-density SS phase for different stabilities of the MS phase ($\Delta\omega_{MS}$). The stability of the MS phase is gradually varied. Note the increased wetting effects upon increasing the stability of the intermediate phase. (B) Dependence of the surface tension of the melt–SS interface on the extent of metastability of the intermediate solid.

surface tension upon increasing the stability of the intermediate phase. This decrease in surface tension is a consequence of the enhanced wetting of the high-density solid interface with an intermediate-density phase.

C. Crossover from Wetting to the OSR. At a particular supersaturation, we can evaluate the nucleation barrier as well as the density profile of the critical nucleus by solving the Euler–Lagrange equations associated with the following condition

$$\frac{\delta\Omega[\rho(r)]}{\delta\rho(r)} = 0 \quad (7)$$

where $\Omega[\rho(r)]$ is the grand canonical free energy functional corresponding to the nucleus of the daughter phase with density profile $\rho(r)$. The density profiles of critical nuclei (shown in Figure 3) are obtained by solving the corresponding Euler–Lagrange equations under appropriate boundary conditions. In order to understand the effects of the intermediate phase on the composition of the critical nucleus, we have fixed the free energy gap (supersaturation) between the parent melt and SS phases and gradually varied the stability of the intermediate (MS) phase with respect to the parent melt ($\Delta\omega_{MS}$). This construction allows us to reveal solely the effect of wetting by the intermediate phase on the composition of the critical nucleus and corresponding energy cost. In contrast, in reality, this effect cannot be quantified directly because the stability of the intermediate phase is varied by changing the supersaturation, which also affects the stability of the SS phase. As a result, we always observe two superimposed effects on the nucleation barrier, wetting by the intermediate phase and the effect due to increased stability of the SS phase.

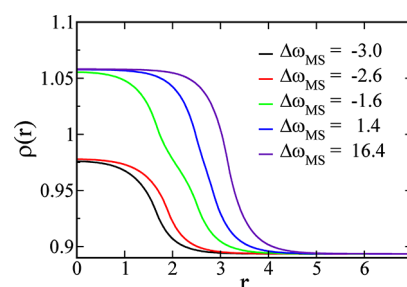


Figure 3. Calculated density profiles of critical nuclei for different stabilities of the intermediate phase at a fixed supersaturation (the free energy difference between the melt and SS phases is kept fixed). Note the sudden change in the density profile below a certain value of $\Delta\omega_{MS}$.

As is evident from Figure 3, at a fixed supersaturation (between the low-density melt and high-density SS), the density profiles for the critical nucleus at different depths (extent of stability with respect to the parent melt) of the intermediate phase are shown. When the intermediate phase has minimal stability with respect to the low-density melt phase, one step density profiles suggest the negligible role of the intermediate phase in the construction of the equilibrium density profile for the critical nucleus of the high-density phase. This indicates the absence of wetting of the nucleus of the high-density phase by the intermediate-density phase. Upon gradually increasing the stability of the intermediate phase, we observe significant deviations in the density profile of the critical cluster of the high-density solid phase. These deviations indicate the change in the composition of the critical cluster of the SS phase by an intermediate solid phase (MS). On further increasing the stability of the intermediate phase, we observe a transition where a critical cluster of the intermediate phase appears inside the bulk metastable melt phase. This is the OSR scenario, where transition from the melt to the final stable phase occurs via many intermediate phases. Thus, upon increasing the stability of the intermediate phase, we observe a crossover from the wetting-enhanced one step transition to the sequential two step (following the OSR) transition.

In Figure 4, we have shown the dependence of the nucleation barrier from the melt to SS and the melt to MS phases on the pressure of the melt phase (supersaturation). At high supersaturation, we note the crossover in the free energy

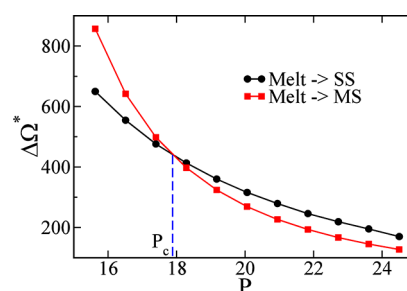


Figure 4. The crossover of the free energy barrier of nucleation upon changing the pressure (P) of the melt phase is shown. The red line with filled squares indicates the free energy barrier of nucleation from the melt to intermediate solid, and the black line with filled circles indicates the transition from the melt to SS. The crossover in the free energy barrier indicates the transition from wetting-mediated nucleation of the SS to the OSR.

barrier for nucleation of the metastable and stable phases. At low supersaturation, the nucleation free energy barrier for the SS phase in the presence of the MS phase is lower than the nucleation barrier for the metastable phase. This is due to the wetting of a cluster of the SS phase by an intermediate MS phase. At low supersaturation, the melt phase directly goes to the SS phase without encountering the bulk MS phase. However, at large supersaturation, the nucleation barrier for the MS phase is lower than that for the SS phase. The melt first undergoes a transition to the MS phase followed by a transition from the metastable to the SS phase (OSR). This crossover is also observed by Oxtoby et al.¹² in the case of one MS phase, although they did not mention explicitly the OSR type scenario. This crossover has important consequences on the pathway of phase transition in many simple and complex systems. In the next section, we shall discuss the more generalized free energy landscape having multiple minima and its effect on pathways of phase transition.

3. MULTIPLE METASTABLE PHASES: SURFACE TENSION AND NUCLEATION BARRIER

A. Surface Tension. In this section, we shall generalize the above discussion for the case of multiple metastable intermediate phases. For simplicity, we have first considered a case of two intermediate phases. A schematic illustration of the complex free energy landscape consisting of two metastable intermediate phases is provided in Figures 5 and 7. In Figure 5,

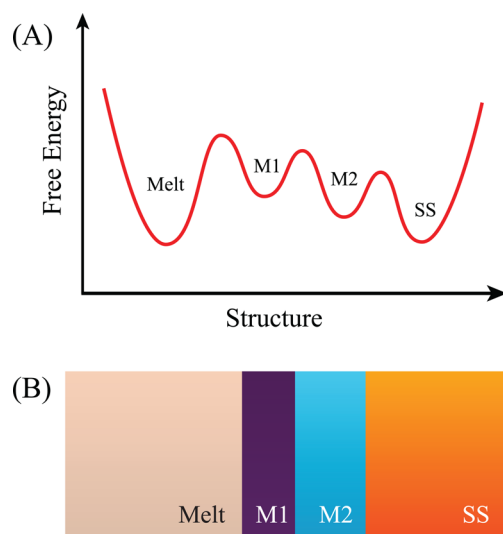


Figure 5. (A) A schematic illustration of a complex energy landscape consisting of two metastable intermediates is shown when the initial melt and final SS phases are at coexistence. (B) A schematic illustration of the planar interface between the melt and SS phases wetted by two intermediate phases M1 and M2 is shown.

we have shown the free energy landscape at a pressure, where the melt and SS phases coexist (Figure 5A) along with a schematic diagram of the interface between the melt and the SS phase at coexistence wetted by two intermediate phases (Figure 5B). In order to study the effects of two intermediate phases using DFT, we have constructed the Helmholtz free energies of different phases (melt, M1, M2, and SS) similar to the one presented in eq 2 with following parameter values: $a_M = 1500$, $a_{M1} = 2000$, $a_{M2} = 2000$, $a_{SS} = 2500$, $\rho_M = 0.88$, $\rho_{M1} = 0.937$,

$\rho_{M2} = 0.992$, $\rho_{SS} = 1.05$, $f_{M,0} = 0.0$, $f_{M1,0} = 0.08$, $f_{M2,0} = 1.0$, and $f_{SS,0} = 0.80$.

In Figure 6, we have plotted the equilibrium density profile for the proposed free energy surface at coexistence of the melt

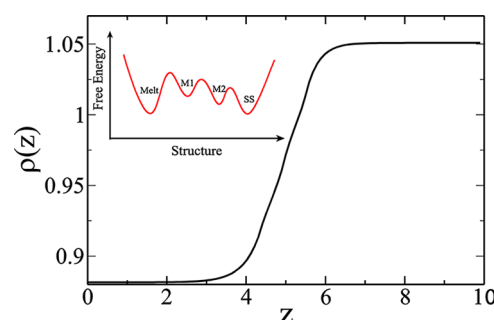


Figure 6. The calculated density profile for the case of two metastable intermediate phases (M1 and M2 and a schematic plot of the free energy are shown in the inset) at coexistence of the melt and SS phases.

and SS phases. The density profile is wetted by two metastable intermediate phases. Similar to the earlier case (the case of one intermediate phase), one would observe an enhanced wetting of the interface upon increasing the stability of the intermediate phases. The width of the intermediate phase participating in the wetting will depend on the stability and position of the respective intermediate phase with respect to coexisting melt or SS phases.

B. Nucleation Barrier. In Figure 7A, we have shown a schematic energy landscape under supersaturated condition. The initial metastable melt and the SS phases are separated by multiple MS (with respect to SS) phases. In the case of two metastable intermediate phases, there can be three possibilities:

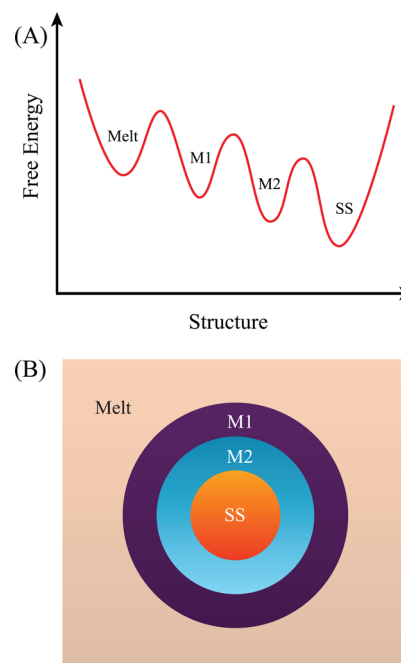


Figure 7. (A) A schematic representation of a complex energy landscape consisting of two metastable intermediates under supersaturated conditions is shown. (B) A growing nucleus wetted by all intermediate phases is shown schematically.

(i) All intermediate phases participate in the wetting of the nucleus of the SS phase in the bulk metastable melt (shown in Figure 7B). (ii) At first, the melt completely transforms to one of the metastable states; however, the other intermediate phase participates in wetting. This is the case of the partial OSR. (iii) The system sequentially moves from the melt to the SS phase via intermediate metastable phases. This is the case of the complete OSR. We must note that in the case of one intermediate, only two scenarios (wetting-induced one step and sequential OSR) are possible.

In order to find the conditions under which we can realize the above-mentioned different cases, we need to compute nucleation barrier with varying supersaturation. In Figure 8, we

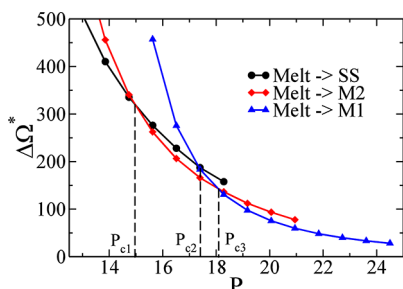


Figure 8. The computed free energy barriers of nucleation of different phases from the melt at different pressures of the melt phase are shown. Note the multiple crossovers at different pressures are indicated by vertical dotted lines (P_{c1} , P_{c2} , and P_{c3}).

have plotted the free energy barrier for nucleation of three different phases, M1, M2, and SS from the metastable melt phase at different pressures of the melt phase. The black line with filled circles indicates the supersaturation-dependent free energy barrier for nucleation of the stable phase in the bulk metastable melt, the red line with filled diamonds indicates the same for the nucleation of M2, and the blue line with filled triangles indicates the same for the nucleation of M1. We note that there are multiple crossovers in the free energy barriers for nucleation of different phases in the melt. This has an important consequence on deciding the pathways of transition and is discussed in detail in the next section.

At low supersaturation (pressure), the free energy barrier for nucleation of SS is lower than that for both M1 and M2. That is, at low supersaturation, the melt phase will directly undergo a transition to the stable phase without encountering any bulk intermediate metastable (M1 and M2) phases. The role of the intermediate phases is to reduce the free energy barrier for the nucleation of the stable phase by wetting. Thus, not encountering a metastable intermediate phase during transition does not discard the possibility of existence of metastable states. Upon increasing the supersaturation, we observe a crossover in the free energy barrier of SS and M2. Beyond the crossover point (P_{c1}), the system will directly undergo a transition to the M2 followed by transition to SS. The critical cluster of M2 is wetted by the M1 phase and thus reduces the free energy barrier for transition to M2. This is the partial OSR scenario where the system is exploring only one intermediate state (M2) before transferring to the final SS. Upon further increasing the supersaturation, we observe another crossover where the nucleation free energy barrier for M1 is lower than that for both M2 and SS. Beyond P_{c3} , the melt will first transform to M1 followed by transformation to other phases (M2 and SS). This way, by modulating the free energy landscape, one can

create a situation where the system will sequentially move from one metastable state to another before moving to the final SS phase. This is the case of the complete Ostwald step rule. However, Ostwald's rule might fail at very large supersaturations, when the size of the critical nucleus is of the size of inhomogeneities of the liquid structure.

The different scenarios (discussed above) indicate that the crystallization pathways are richer than the predictions of the OSR and depend on many factors such as the number, well depths, and positions of the free energy minima of the intermediate phases. The well depths and positions of the free energy minima can be tuned easily by changing the thermodynamic parameters such as temperature and pressure. The number of intermediate phases depends on the system under consideration. Thus, the change of thermodynamic parameters has a profound effect on the selection of the pathways of the crystallization. Recently, Whitlam and co-workers³⁹ have also observed a rich crystallization pathway in the case of a patchy colloidal model system.

C. Dependence of the Surface Tension on Multiple Intermediate Phases Coexisting with Each Other. In this section, we shall discuss the dependence of surface tension on the number of intermediate coexisting phases. The initial melt and final SS phase are separated by N coexisting intermediate phases. The grand potential density difference (relative to the bulk initial phase) of the melt ($\Delta\omega_M$), i th intermediate ($\Delta\omega_i$), and SS phase ($\Delta\omega_{SS}$) is given as

$$\begin{aligned}\Delta\omega_M &= \frac{1}{2}k(\rho - \rho_M)^2 \\ \Delta\omega_i &= \frac{1}{2}k(\rho - \rho_i)^2 \\ \Delta\omega_{SS} &= \frac{1}{2}k(\rho - \rho_{SS})^2\end{aligned}\quad (8)$$

where for simplicity we have assumed that the curvatures of the free energy surfaces are same for all phases. ρ_M and ρ_{SS} are the equilibrium densities of the melt and SS phase, respectively. ρ_i is the equilibrium density of the i th intermediate phase and is given as $\rho_M + i\Delta\rho$, where $\Delta\rho = (\rho_{SS} - \rho_M)/(N + 1)$. Following Cahn–Hilliard,⁴⁰ the work of formation of the critical nucleus is given as

$$\Omega = \int d\mathbf{r} [\Delta\omega(\rho(\mathbf{r})) + c(\nabla\rho)^2] \quad (9)$$

where c is related to the correlation length. Using the analytical expression of the surface tension originally derived by Cahn and Hilliard,⁴⁰ $\gamma = 2\sqrt{c} \int_{\rho_i}^{\rho_f} (\Delta\omega)^{1/2} d\rho$, a relation between the wetted surface tension ($\gamma_{M/SS}^w$) and that without wetting ($\gamma_{M/SS}$), can be easily derived and is given as

$$\gamma_{M/SS}^w = \gamma_{M/SS} \frac{2N + 1}{(N + 1)^2} \quad (10)$$

where $\gamma_{M/SS} = [(2kc)^{1/2}/4](\rho_{SS} - \rho_M)^2$; here, c is the coefficient of the square gradient term, and k is the curvature of the grand potential. From the above expression, it is quite evident that for larger N , the surface tension decreases as the inverse of N , and as discussed earlier, this has an important consequence on the nucleation and growth processes in complex systems.

4. GENERALIZED FREE ENERGY FUNCTIONAL: TWO ORDER PARAMETER DESCRIPTION

For crystallization, a two order parameter (density and order) description is often necessary. For simplicity, we consider the case with only one intermediate metastable solid phase (referred as MS) between the fluid (melt) and final stable solid (SS). We follow Oxtoby in describing the free energy functional of the inhomogeneous phase, characterized by position-dependent order parameters.³⁸ The proposed free energy functionals for three phases, fluid (F), intermediate MS, and SS are

$$\Omega_i[\rho(\mathbf{r}), m(\mathbf{r})] = \int d\mathbf{r} [f_i(\rho(\mathbf{r}), m(\mathbf{r})) - \mu\rho(\mathbf{r})] + \frac{1}{2} \int d\mathbf{r} [K_{\rho i}(\nabla\rho(\mathbf{r}))^2] + \frac{1}{2} \int d\mathbf{r} [K_{m i}\rho_s^2(\nabla m(\mathbf{r}))^2] \quad (11)$$

where f_i is a local Helmholtz free energy density function of the average number density $\rho(\mathbf{r})$ and structural order parameter $m(\mathbf{r})$ and μ is the chemical potential. Here, i indicates respective phases. The square gradient terms account for the nonlocal effects in the system due to inhomogeneity in the density and structural order parameters. $K_{\rho i}$ and $K_{m i}$ are related to correlation lengths for ρ and m . Following Talanquer and Oxtoby,³⁸ the Helmholtz free energy density for the homogeneous fluid is

$$f_f(\rho, m) = k_B T \rho [\ln \rho - 1 - \ln(1 - b\rho)] - a\rho^2 + k_B T \alpha_1 m^2 \quad (12)$$

The above free energy functional is a generalization of van der Waal's free energy functional for a two order parameter description. In a similar spirit, one can also write the Helmholtz free energy functional for solids (metastable and stable) as

$$f_j(\rho, m) = k_B T \rho [\ln \rho - 1 - \ln(1 - b\bar{\rho})] - a\rho^2 + k_B T [\alpha_1 j m^2 + \alpha_2 j] \quad (13)$$

where $j = \text{MS}$ for the metastable intermediate solid and SS for the stable solid. Here, k_B is the Boltzmann's constant, T is the absolute temperature, and a and b are the van der Waal's parameters. $\bar{\rho}$ is the weighted average density and is given as

$$\bar{\rho} = \rho[1 - \alpha_3 m(\alpha_4 j - m)] \quad (14)$$

The values of the parameters are $a = 1.0$, $b = 1.0$, $\alpha_1 = \alpha_{1\text{MS}} = \alpha_{1\text{SS}} = 0.25$, $\alpha_{2\text{MS}} = 1.5$, $\alpha_{3\text{MS}} = 0.22$, $\alpha_{4\text{MS}} = 1.85$, $\alpha_{2\text{SS}} = 2.0$, $\alpha_{3\text{SS}} = 0.30$, $\alpha_{4\text{SS}} = 2.0$, $K_{\rho i} = a/2$, and $K_{m i} = a/8$. A contour plot of free energy functions given by eqs 12 and 13 are shown in Figure 9.

A. Phase Diagram. The density and structural order of coexisting phases can be determined by equating the chemical potential and thermodynamic grand potential density (pressure) of the two phases.

$$\mu_\alpha(\rho_\alpha) = \mu_\beta(\rho_\beta) \quad \text{and} \quad \omega_\alpha(\rho_\alpha) = \omega_\beta(\rho_\beta) \quad \text{where} \quad \mu_i = \left(\frac{\partial f_i(\rho, m)}{\partial \rho} \right)_T \quad \text{and} \quad \omega_i = f_i - \mu_i \rho_i \quad (15)$$

The above two conditions ensure that the system is in both thermodynamic and mechanical equilibrium. Figure 10 shows the results of quantitative calculation of the coexistence

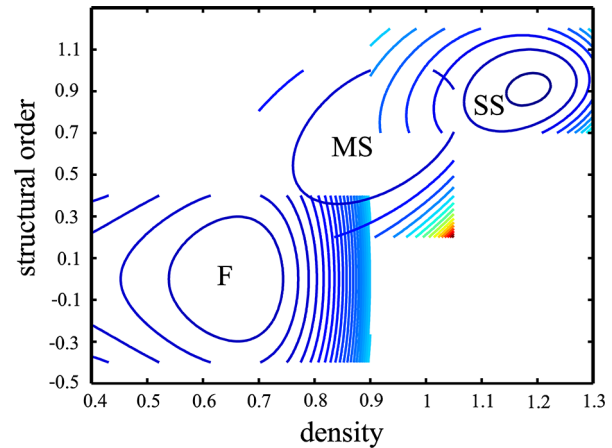


Figure 9. A contour diagram of two-dimensional free energy surfaces given by eqs 12 and 13 is shown. F stands for the fluid phase, MS for the metastable intermediate solid, and SS for the stable solid.

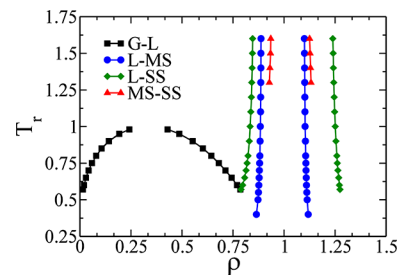


Figure 10. The computed phase diagram for the proposed free energy surfaces at reduced temperature $T_r = T/T_c$. The black lines (with squares) indicate the gas–liquid coexistence. Green lines (with diamonds) indicate the coexistence between the F and SS, and blue lines (with circles) indicate the coexistence between the F and MS. Red lines (with triangle up) indicate the coexistence between the intermediate MS and SS.

between gas–liquid, liquid–intermediate MS (L–MS), liquid–SS (L–SS), and MS and SS. As gas–liquid interfacial surface tension depends strongly on the order parameter difference, and one can qualitatively conclude that the surface tension between the fluid and SS will be larger than that between the fluid and MS phase. More accurate quantitative results of the interfacial surface tension between fluid–MS and fluid–SS are discussed in the next section.

B. Surface Tension. For the phase diagram shown in Figure 10, we can evaluate the values of the surface tension between the coexisting phases (L–SS and L–MS) for a planar interface along the z -axis by solving the Euler–Lagrange equations associated with following equilibrium conditions

$$\frac{\delta\Omega}{\delta\rho(z)} = 0 \quad \text{and} \quad \frac{\delta\Omega}{\delta m(z)} = 0 \quad (16)$$

where $\Omega(\rho(z), m(z))$ is the grand canonical free energy functional corresponding to the inhomogeneous system with density profile $\rho(z)$ and order profile $m(z)$

$$\Omega[\rho(z), m(z)] = \int dz [f(\rho(z), m(z)) - \mu\rho(z)] + \frac{1}{2} \int dz [K_\rho(\nabla\rho(z))^2] + \frac{1}{2} \int dz [K_m\rho_s^2(\nabla m(z))^2] \quad (17)$$

Here, $f = \min\{f_{ij}\}$.

Upon minimizing the above free energy functional with respect to density and order profiles (or equivalently, solving the corresponding Euler–Lagrange equations under appropriate boundary conditions), we obtain the equilibrium density and order profiles. Equilibrium density and order profiles for L–MS and L–SS interfaces are shown in Figure 11. The

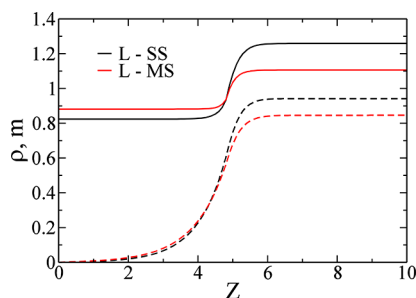


Figure 11. The calculated density and order profile for the planar interface along the z -axis at $T_r = 0.80$. Solid lines indicate the density profiles along L–SS and L–MS interfaces. Dotted lines indicate the order profiles along L–SS and L–MS interfaces.

surface tension is extra free energy cost for the formation of an interface and is defined as

$$\gamma_{i/j} = \frac{(\Omega(\rho(z), m(z)) - \Omega_{i/j})}{A} \quad (18)$$

where $\Omega_{i/j}$ is the free energy of the coexisting i th and j th phases and A is the area of the interface. The calculated surface tension values (using eqs 17 and 18) for L–MS and L–SS at coexistence are $\gamma_{L/MS} = 6.8 \times 10^{-2}$ and $\gamma_{L/SS} = 14.7 \times 10^{-2}$ (in units of $a/b^{5/3}$).

If we consider the free energy landscape shown in Figure 7A as a representative of metastable crystallization, the free energy difference between different phases will follow the trend, in general, $\Delta G_{LM1} < \Delta G_{LM2} < \dots < \Delta G_{LSS}$, and the above theoretical analysis suggests that the surface tension would follow $\gamma_{LM1} < \gamma_{LM2} < \dots < \gamma_{LSS}$. Physically, it can be understood that less energy is required for formation of disordered or open structured low-density solids from the melt or sol phase.

5. KINETIC SCHEME: VANISHING POLYMORPHS

In this section, we shall briefly discuss the kinetic equations for phase transformation in the presence of *one* metastable phase. Let P_M , P_{MS} , and P_{SS} denote the population of the metastable melt, MS, and SS phases, respectively.

$$\begin{aligned} \frac{\partial P_M(r, t)}{\partial t} &= -k_{M \rightarrow MS}(r)P_M + k_{MS \rightarrow M}(r)P_{MS} \\ \frac{\partial P_{MS}(r, t)}{\partial t} &= -k_{MS \rightarrow M}(r)P_{MS} - k_{MS \rightarrow SS}(r)P_{MS} + k_{M \rightarrow MS}(r)P_M \\ &\quad + k_{SS \rightarrow MS}(r)P_{SS} - k_{pMS}(r)P_{MS} \\ \frac{\partial P_{SS}(r, t)}{\partial t} &= -k_{SS \rightarrow MS}(r)P_{SS} + k_{MS \rightarrow SS}(r)P_{MS} - k_{pSS}(r)P_{SS} \end{aligned} \quad (19)$$

where k_{pMS} is the size-dependent precipitation rate of metastable phase of size r and k_{pSS} is the precipitation rate of the SS phase. These kinetic equations have very close resemblance with the sequential chemical reactions in the presence of a sink term. However, this analogy is only partial. In the case of phase transition, we do not require fulfillment of the

detailed balance condition as a metastable phase cannot grow inside of a stable phase. Thus, in the above generalized kinetic equation, the rate constants for back reactions will only be effective in the case of a weak first-order transition (where the free energy barrier for the back reaction is very small and the system can move collectively toward the metastable phase). In other cases, back reaction rate constants will be zero. We should also note that contrary to the case of reaction dynamics, in the phase transition, the system overcomes not the global free energy barrier but the local nucleation free energy barrier due to surface tension.

Solution of eq 19 needs values of size-dependent rate constants. The size dependence of the rate shall have a crossover if we start from small, precritical sizes. They shall clearly depend on the degree of supersaturation. If we further assume that the rate-limiting step is the nucleation step, then these transition rates can be obtained from the nucleation rate calculated here. The rates of precipitation are a bit more difficult to estimate and shall clearly depend on the size of the growing cluster. One could imagine a crossover in the size dependence here too. In a general scheme, these clusters should interact with each other but are neglected here. If we neglect the precipitation and the intercluster interaction effects, then the following scenario unfolds. When the intermediate states are metastable with respect to both the parent liquid and the final SS, the intermediate phases will not nucleate and shall not form but only wet the interface. Macroscopic observation might not find any signature of the metastable phases as their only signature will be at the interface. Solution of eq 19 then shall have the zero rates of formation for the metastable phases, but their “hidden” effect will be in enhancing $k_{M \rightarrow SS}$, which is the rate of formation of SS from the melt. In this paper, we have called this the wetting-dominated regime.

However, when the intermediate phases are of lower free energy than the parent liquid but metastable with respect to the SS phase, then one may be able to detect/isolate these phases. We have called this the OSR-dominated regime. However, here, also their appearance may be short-lived if the free energy gap between them and the SS is large and that between them and metastable liquid is small. Thus, one shall find the appearance of vanishing polymorphs, often discussed in the literature.

6. CONCLUSION

In KTW and XW¹ treatment of nucleation of a liquid from a glass phase, wetting leads to a size-dependent surface tension, and the nucleation barrier decreases as the size of the nucleus grows. In that case, both the parent (glass) and daughter (liquid) phases are disordered and differ at the thermodynamic (macroscopic) scale only by entropy. Therefore, the precise quantification of the intermediate phases is left a bit unclear, although the results appear to be robust. The size of the critical nucleus scales as $s_c^{-2/3}$, and the activation barrier goes as $1/s_c$ (Adam–Gibbs relation). In the mosaic picture of the liquid–glass transition, the system is dynamically inhomogeneous, with regions characterized by different entropies and dynamical properties. Configurational entropy serves as an order parameter with certain similarity with Marcus theory where energy is the order parameter.

In the present scenario of the growth of a new phase from melt, the situation is more clear. We employ an order parameter description with distinct intermediate states, and we show that the surface tension inevitably decreases in the presence of metastable intermediate phases, and also, the free

energy barrier of nucleation decreases. We find that, depending on the number, depth, and location of the free energy minima of intermediate phases between the parent and final phases, a great variety of situations can arise, and this appears to be in general conformity with Ostwald's original hypothesis.

Unfortunately, our information about free energy surfaces of the complex systems often studied in experiments is rather poor. Therefore, in this work, we have to constrain at a highly general picture. We have shown that within the DFT approach, the surface tension decreases as $1/N$ (N is the number of intermediate phases). However, the relation between the size of the critical nucleus and the surface tension remains a bit tricky as we find that the width of the interface is sensitive to many factors.

In conclusion, we have investigated, motivated by the pioneering work of Wolynes and Co-workers,¹ the influence of wetting in kinetics of first-order phase transformations and provide theoretical justification of the phenomena often described by the OSR. We hope to extend the present study to evolve a more quantitative description of specific systems.

One important problem where the present ideas can find use is the much discussed crystallization of supercooled water at 231 K observed by Speedy and Angel⁴¹ in 1972. While much discussion has focused on the possible existence (or absence) of a high-density liquid (HDL)–low-density liquid (LDL) critical point, less attention has focused on crystallization.^{42,43} The present work suggests that nucleation of ice can be facilitated either by wetting of the HDL–ice interface by LDL, if LDL is indeed a metastable minimum in the order parameter space. In the alternate scenario of a critical point between HDL and LDL, the large-scale fluctuations can lower the free energy barrier, as observed not too long ago by ten Wolde and Frenkel in the case of protein crystallization.⁴⁴ The large-scale fluctuations near a submerged critical point may be detected otherwise as the variation of specific heat near the Widom line. From the effects on the free energy barrier, it is hard to distinguish between the two scenarios as both can facilitate nucleation of ice. Only if we could study the nucleus near its critical size, we could make a distinction between the two. Nevertheless, existence of a metastable phase, like LDL water, with an order intermediate between the HDL and ice can greatly facilitate nucleation of ice from HDL water. Computer simulation studies of freezing of water^{42,43,45} do seem to indicate that ice nucleates from LDA-like regions. In fact, the presence of a metastable liquid or solid phase with intermediate order can even facilitate nucleation to such an extent that the phase transition may even look like a spinodal decomposition or the limit of stability of the liquid phase.

AUTHOR INFORMATION

Corresponding Author

*E-mail: bbagchi@sscu.iisc.ernet.in.

Notes

The authors declare no competing financial interest.

ACKNOWLEDGMENTS

We thank Professor C. N. R. Rao and Professor J. Gopalakrishnan for helpful discussions. This work was supported in parts by grants from BRNS and DST. B.B. acknowledges support from a JC Bose Fellowship (DST).

REFERENCES

- (1) (a) Kirkpatrick, T. R.; Thirumalai, D.; Wolynes, P. G. Scaling Concepts for the Dynamics of Viscous Liquids near an Ideal Glassy State. *Phys. Rev. A* **1989**, *40*, 1045–1054. (b) Xia, X.; Wolynes, P. G. Fragilities of Liquids Predicted from the Random First Order Transition Theory of Glasses. *Proc. Natl. Acad. Sci. U.S.A.* **2000**, *97*, 2990–2994.
- (2) Adam, G.; Gibbs, J. H. On the Temperature Dependence of Cooperative Relaxation Properties in Glass-Forming Liquids. *J. Chem. Phys.* **1965**, *43*, 139–146.
- (3) ten Wolde, P. R.; Ruiz-Montero, M. J.; Frenkel, D. Numerical Evidence for bcc Ordering at the Surface of a Critical fcc Nucleus. *Phys. Rev. Lett.* **1995**, *75*, 2714–2717.
- (4) ten Wolde, P. R.; Frenkel, D. Homogeneous Nucleation and the Ostwald Step Rule. *Phys. Chem. Chem. Phys.* **1999**, *1*, 2191–2196.
- (5) Alexander, S.; McTague, J. Should All Crystals Be bcc? Landau Theory of Solidification and Crystal Nucleation. *Phys. Rev. Lett.* **1978**, *41*, 702–705.
- (6) Russo, J.; Tanaka, H. The Microscopic Pathway to Crystallization in Supercooled Liquids. *Sci. Rep.* **2012**, *2*, 505–512.
- (7) Russo, J.; Tanaka, H. Selection Mechanism of Polymorphs in the Crystal Nucleation of the Gaussian Core Model. *Soft Matter* **2012**, *8*, 4206–4215.
- (8) Kawasaki, T.; Tanaka, H. Formation of a Crystal Nucleus from Liquid. *Proc. Natl. Acad. Sci. U.S.A.* **2010**, *107*, 14036–14041.
- (9) Van Santen, R. A. The Ostwald Step Rule. *J. Phys. Chem.* **1984**, *88*, 5768–5769.
- (10) Ostwald, W. Studien über die Bildung und Umwandlung fester Körper. *Z. Phys. Chem.* **1897**, *22*, 289–330.
- (11) Stranski, I. N.; Totomanow, D. Rate of Formation of (Crystal) Nuclei and the Ostwald Step Rule. *Z. Phys. Chem.* **1933**, *163*, 399–408.
- (12) Granasy, L.; Oxtoby, D. W. Cahn–Hilliard Theory with Triple-Parabolic Free Energy. II. Nucleation and Growth in the Presence of a Metastable Crystalline Phase. *J. Chem. Phys.* **2000**, *112*, 2410–2419.
- (13) Sikkenk, J. H.; Van Leeuwen, J. M. J.; Vossnack, E. O.; Bakker, A. F. Simulation of a Liquid–Vapor Interface in an External Field. *Physica A* **1987**, *146*, 622–633.
- (14) Lubchenko, V.; Wolynes, P. G. Theory of Structural Glasses and Supercooled Liquids. *Annu. Rev. Phys. Chem.* **2007**, *58*, 235–266.
- (15) Bryngelson, J. D.; Onuchic, J. N.; Socci, N. D.; Wolynes, P. G. Funnels, Pathways, and the Energy Landscape of Protein Folding: A Synthesis. *Proteins: Struct., Funct., Genet.* **1995**, *21*, 167–195.
- (16) Chung, S. Y.; Kim, Y. M.; Kim, J. G.; Kim, Y. J. Multiphase Transformation and Ostwald's Rule of Stages During Crystallization of a Metal Phosphate. *Nat. Phys.* **2009**, *5*, 68–73.
- (17) Wales, D. J. *Energy Landscapes: Applications to Clusters, Biomolecules and Glasses*; Cambridge University Press: New York, 2003.
- (18) Frauenfelder, H.; Sligar, S. G.; Wolynes, P. G. The Energy Landscapes and Motions of Proteins. *Science* **1991**, *254*, 1598–1603.
- (19) Ramakrishnan, T. V.; Yussouf, M. First-Principles Order-Parameter Theory of Freezing. *Phys. Rev. B* **1977**, *19*, 2775–2794.
- (20) (a) Davis, M. E.; Lobo, R. F. Zeolite and Molecular Sieve Synthesis. *Chem. Mater.* **1992**, *4*, 756–768. (b) Petrovic, I.; Navrotsky, A.; Davis, M. E.; Zones, S. I. Thermochemical Study of the Stability of Frameworks in High Silica Zeolites. *Chem. Mater.* **1993**, *5*, 1805–1813. (c) Henson, N. J.; Cheetham, A. K.; Gale, J. D. Theoretical Calculations on Silica Frameworks and Their Correlation with Experiment. *Chem. Mater.* **1994**, *6*, 1647–1650.
- (21) (a) Debenedetti, P. G. *Metastable Liquids: Concepts and Principles*; Princeton University Press: Princeton, NJ, 1996. (b) Frenkel, J. *Kinetic Theory of Liquids*; Dover: New York, 1955. (c) Zettlemoyer, A. C. *Nucleation*; Dekker: New York, 1969.
- (22) Becker, R.; Döring, W. Kinetische Behandlung der Keimbildung in übersättigten Dämpfen. *Ann. Phys.* **1935**, *24*, 719–752.
- (23) Debenedetti, P. G. Thermodynamics: When a Phase is Born. *Nature* **2006**, *441*, 168–169.

- (24) Langer, J. S. Theory of Condensation Point. *Ann. Phys.* **1967**, *41*, 108–157.
- (25) Oxtoby, D. W. Crystallization: Diversity Suppresses Growth. *Nature* **2001**, *413*, 694–695.
- (26) Binder, K. “Clusters” in the Ising Model, Metastable States and Essential Singularity. *Ann. Phys.* **1976**, *98*, 390–417.
- (27) Bhimalapuram, P.; Chakrabarty, S.; Bagchi, B. Elucidating the Mechanism of Nucleation near the Gas–Liquid Spinodal. *Phys. Rev. Lett.* **2007**, *98*, 206104–206107.
- (28) Santra, M.; Bagchi, B. Crossover Dynamics at Large Metastability in Gas–Liquid Nucleation. *Phys. Rev. E* **2011**, *83*, 031602–031608.
- (29) Santra, M.; Singh, R. S.; Bagchi, B. Gas–Liquid Nucleation at Large Metastability: Unusual Features and a New Formalism. *J. Stat. Mech.* **2011**, P03017.
- (30) Maibaum, L. Phase Transformation near the Classical Limit of Stability. *Phys. Rev. Lett.* **2008**, *101*, 256102–256105.
- (31) ten Wolde, P. R.; Frenkel, D. Computer Simulation Study of Gas–Liquid Nucleation in a Lennard-Jones System. *J. Chem. Phys.* **1998**, *109*, 9901–9918.
- (32) Trudo, F.; Donadio, D.; Parrinello, M. Freezing of a Lennard-Jones Fluid: From Nucleation to Spinodal Regime. *Phys. Rev. Lett.* **2006**, *97*, 105701–105704.
- (33) Stillinger, F. H.; Buff, F. P. Equilibrium Statistical Mechanics of Inhomogeneous Fluids. *J. Chem. Phys.* **1962**, *37*, 1–12.
- (34) Lebowitz, J. L.; Percus, J. K. Statistical Thermodynamics of Nonuniform Fluids. *J. Math. Phys.* **1963**, *4*, 116–123.
- (35) Evans, R. The Nature of the Liquid–Vapour Interface and Other Topics in the Statistical Mechanics of Non-Uniform, Classical Fluids. *Adv. Phys.* **1979**, *28*, 143–200.
- (36) Oxtoby, D. W.; Evans, R. Nonclassical Nucleation Theory for the Gas–Liquid Transition. *J. Chem. Phys.* **1988**, *89*, 7521–7530.
- (37) Shen, Y. C.; Oxtoby, D. W. bcc Symmetry in the Crystal–Melt Interface of Lennard-Jones Fluids Examined through Density Functional Theory. *Phys. Rev. Lett.* **1996**, *77*, 3585–3588.
- (38) Talanquer, V.; Oxtoby, D. W. Crystal Nucleation in the Presence of a Metastable Critical Point. *J. Chem. Phys.* **1998**, *109*, 223–227.
- (39) Hedges, L. O.; Whitelam, S. Limit of Validity of Ostwald’s Rule of Stages in a Statistical Mechanical Model of Crystallization. *J. Chem. Phys.* **2011**, *135*, 164902–164907.
- (40) Cahn, J. W.; Hilliard, J. E. Free Energy of a Nonuniform System. I. Interfacial Free Energy. *J. Chem. Phys.* **1958**, *28*, 258–267.
- (41) Speedy, R. J.; Angel, C. A. Isothermal Compressibility of Supercooled Water and Evidence for a Thermodynamic Singularity at -45°C . *J. Chem. Phys.* **1976**, *65*, 851–858.
- (42) Matsumoto, M.; Saito, S.; Ohmine, I. Molecular Dynamics Simulation of the Ice Nucleation and Growth Process Leading to Water Freezing. *Nature* **2002**, *416*, 409–413.
- (43) Moore, E. B.; Molinero, V. Structural Transformation in Supercooled Water Controls the Crystallization Rate of Ice. *Nature* **2011**, *479*, 506–508.
- (44) ten Wolde, P. R.; Frenkel, D. Enhancement of Protein Crystal Nucleation by Critical Density Fluctuations. *Science* **1997**, *277*, 1975–1978.
- (45) It should be noted that formation of ice from supercooled water is quite sensitive to the force field used. This has often led to uncertainty and even conflicting results.